Ann. Géophys., t. 36, fasc. 3, 1980, p. 323-332

Waves observed by the Araks experiments : generalities

by

J. LAVERGNAT(1), M. DECHAMBRE(1), R. PELLAT(2)
Yu. V. KUSHNEREVSKY(3), S.A. PULINETS(3)

ABSTRACT. – *This paper is devoted to a general presentation of the wave observed by the Araks experiments. One of the main objectives assigned to these experiments was to observe waves generated by an electron beam and its subsequent interaction with the ionosphere. Two kinds of measurements have been made : measurements which led us to know the parameters of the medium (plasma frequency, electronic gyrofrequency, DC electric field, electronic temperature) and measurements related with the injection of an electron beam (plasma mode, whistler mode and the VLF range). This paper relates the main results which have been found. They are discussed more precisely in other papers of this issue.*

RESUME. – *Cet article est consacré à une présentation générale des mesures d'ondes effectuées lors des expériences Araks. L'un des principaux objectifs de ces expériences était d'observer les ondes créées par un faisceau d'électrons et par interaction de celui-ci avec l'ionosphère. Deux types de mesures ont été faits : des mesures conduisant à connaître les paramètres caractéristiques du milieu (fréquence plasma, gyrofréquence électronique, champs électriques continus, température électronique), et des mesures directement liées à l'injection des électrons (mode plasma et mode sifflement dans la gamme HF et la gamme TBF). Il ne s'agit ici que d'un résumé des observations faites et qui sont discutées en détail dans d'autres articles.*

Introduction

One of the main objectives assigned to the Araks experiments was to observe the radio waves generated by the electron beam and the effects of wave-particle interactions on the beam itself. A cone ejected from the main payload (electron gun) carried antennas to detect radio waves created by the electron beam and its subsequent interaction with the ionosphere. Moreover, ground-based measurement facilities were set up, specially VLF and VHF measurements both at the launching site (Kerguelen Islands) and in the Northern hemisphere at its magnetically conjugate point. In the VLF range, no definite observations related to the injection of electrons have been recognized, so we will report nothing else on this matter in this issue. On the other hand many important results have been obtained in the VHF range which seem directly related to the neutralization problem. They will be the subject of a special paper (Mishin and Ruzhin, 1980).

Apart from the waves many other parameters (electric field, temperature, etc. . .) have been measured on the nose cone. Some of these parameters are of primary importance to understand the physical processes involved in the injection of an electron beam into the ionosphere. Thus, we will discuss in details the related observations. Then, we will introduce the observation of the waves themselves leaving the detailed descriptions and discussion to three forthcoming papers each of them being devoted to a definite frequency range (plasma frequency, whistlers and VLF).

(1) Laboratoire de Géophysique Externe, 4 avenue de Neptune, 94100 Saint-Maur des Fossés, France.
(2) Centre de Physique Théorique, Ecole Polytechnique, 91128 Palaiseau Cedex, France.
(3) Institute of Terrestrial Magnetism, Ionosphere and Radio wave Propagation, U.S.S.R. Academy of Sciences, Troitsk, Moscow Region, USSR.

Experimental set-up

The band of frequencies to be received ranges from zero to the upper hybrid frequency at about 5 MHz. To study the polarization, the electric and magnetic components must be measured separately, that was achieved only for frequencies lower than 100 kHz. Figure 1 shows the arrangement of the instruments in the nose cone.

Two small magnetic antennas are mounted on a platform in the upper part of the nose cone. They cover the 1 to 100 kHz band in two subbands : 1 to 10 kHz and 7 to 100 kHz. At the upper end of the nose cone two booms are mounted which carry two vitreous carbon spheres to detect waves in the frequency range from 0 to 100 kHz. The wave electric component, from 100 kHz up to 5 MHz is received with a conventional dipole, 8 m tip-to-tip. Figure 2 shows the simplified block diagram of the complete wave experiment. Detailed descriptions are available in Gusev *et al.* (1978) for the Soviet part (the broad-band telemetry called "SPECTRUM") and in Delahaye *et al.* (1978) for the French part. Matching with the telemetry channel implies some on board data processing which is summarized in Table 1.

Considering the results of Electron Echo 1 and the small distance between the cone and the magnetic field line passing through the rocket the risk of very high values of emission near the plasma frequency at the beginning of the North flight has been anticipated; thus we have set up a 20 dB attenuator at the input of the receiver which was removed 206 sec after the launch.

For the HF part of the waves (0.1-5 MHz) some redundancy can be achieved but the broad band receiver gives more easily very good frequency and time resolution contrary to the narrow band one (sweep frequency analyser) which is limited even if we assume stationary

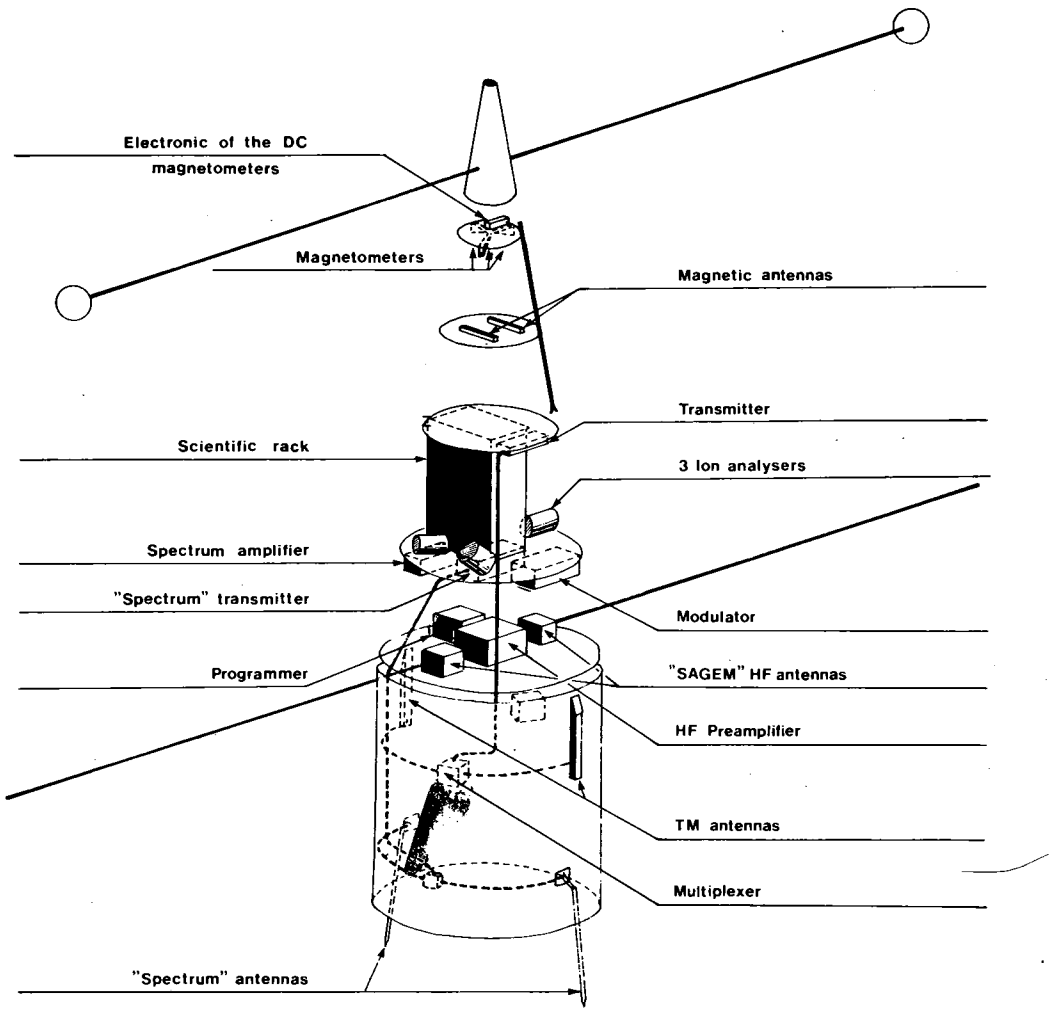

Fig. 1
Arrangement of the nose cone scientific equipment

Table 1

Signal processing systems requirements

Probe	Frequency	Sensitivity	Signal processing	Scientific purpose
Miscellaneous				
Ion current analyser	DC			high induced electric field ion temperature
Probe sheath impedances				Electron temperature
Relaxation	0.1-5 MHz	10^{-8} V Hz$^{-1/2}$	Step analysis	Electron density
Dispersion $f < f_{HB}$	1-6 kHz			Perpendicular distance to B_0
Magnetic Part				
Hall effect magnetometer	< 10 Hz		Waveform	Attitude restitution
Negative flux feedback magnetic probe	10-50 Hz	3×10^{-3} γ	Waveform	Induced magnetic field. Perpendicular distance
Negative flux feedback magnetic probe	1-10 kHz 7-100 kHz	2×10^{-6} γ Hz$^{-1/2}$ 15×10^{-6} γHz$^{-1/2}$	Waveform Frequency step analyser B = 2.25 kHz	Local noise Local noise
Electric Part				
Spherical probes (4 m apart)	0.2-5 Hz 10-50 Hz	10^{-3} V 5×10^{-6} V	Waveform Waveform	Low DC electric field Induced electric field Perpendicular distance
	0.5-10 kHz 7-100 kHz	4×10^{-8} V Hz$^{-1/2}$	Waveform Frequency analysis B = 42.5 kHz	Local noise Local noise
Dipole antenna (2 x 4 m)	0.1-5 MHz	10^{-8} V Hz$^{-1/2}$	Frequency analysis B = 42.5 kHz	Local noise
	2.08-2.28 MHz	10^{-8} V Hz$^{-1/2}$	Detection	Noise around 1.74 f_c high time resolution

signals over 1.28 sec (42.5 kHz and 0.6 msec). The main advantages of the SFA are the large signal to noise ratio and the ease with which the data reduction and statistical analysis are done. To prevent too much interferences from "SPECTRUM" which uses a very high transmitting power, this experiment was switched on during the even sequences only. Electronic density measurements have been performed by the use of a relaxation method.

The resonances are excited throught the dipole antenna by a 31.25 μsec pulse modulated radiofrequency. The receiver is locked during 62.5 μsec around the emission but immediately after the antenna is linked to the receiver tuned on the emitted frequency during 10 msec.

Afterwards the frequency is increased by 38.6 kHz. To cover the whole frequency range 0.1-5 MHz, 128 steps are needed.

A crude estimate of the electronic temperature is obtained by measuring the sheath impedance of the spheres. The preamplifier input resistance is commutated between a very high value (> 10 MΩ) and a moderate one (100 kΩ). Assuming stationary signals

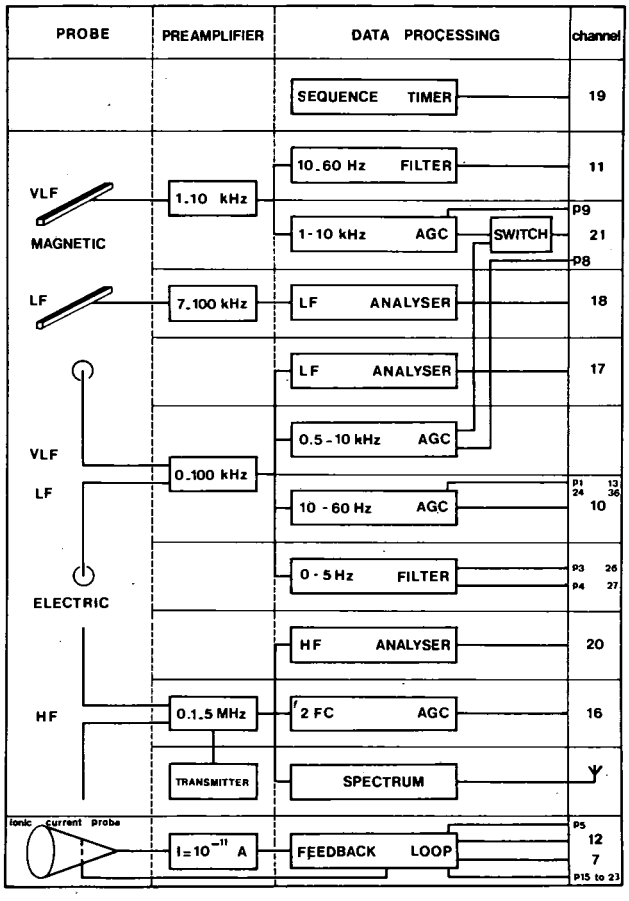

Fig. 2
Experimental system block diagram

the sheath impedance is simply related to the gains g of the two configurations by the following formula :

$$\left|Z_s\right| = 100 \left(\frac{g_1}{g_2} - 1\right) \text{k}\,\Omega.$$

Miscellaneous results

1. Relaxation sounding

As quoted by many authors (e.g. Petit, 1972) the relaxation method gives access to many resonances of the surrounding plasma. In our case, as expected, we have easily identified the plasma resonance f_p and the double of the electronic gyro-frequency f_b (Fig. 3). Some other resonances have been noted such as the upper hybrid resonance (East flight when $f_p < 2f_b$). Figure 4 shows the variations of the observed resonances during both flights. Plasma frequency resonances exhibit a well pronounced maximum near the culmination of the nose cone and the values are in good agreement with those obtained from the ionograms before and after the launch (see the general paper of this issue). The absence of the plasma resonance in the beginning of the North flight can be interpreted as a consequence of the 20 dB attenuation of the HF receiver during this part of the flight (see above).

The results concerning the double of the gyrofrequency are stranger. On Figure 4, the resonances are drawn with their error bars which are close to the band of the receiver ($\simeq$ 40 kHz). Values of the geomagnetic field up to 200 km are predicted with a very good accuracy ($< \pm$ 50 γ for each component) leading

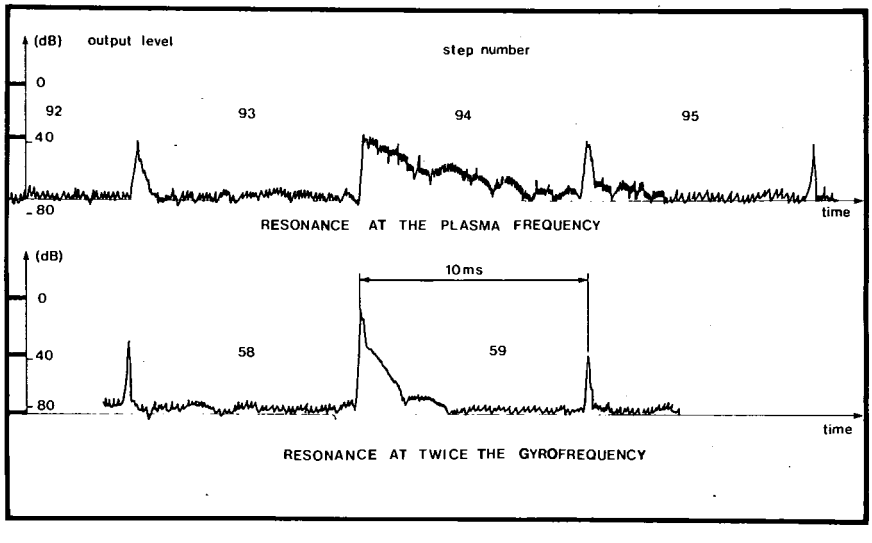

Fig. 3
Examples of resonances seen at the output of the SFA when relaxation sounding is working.

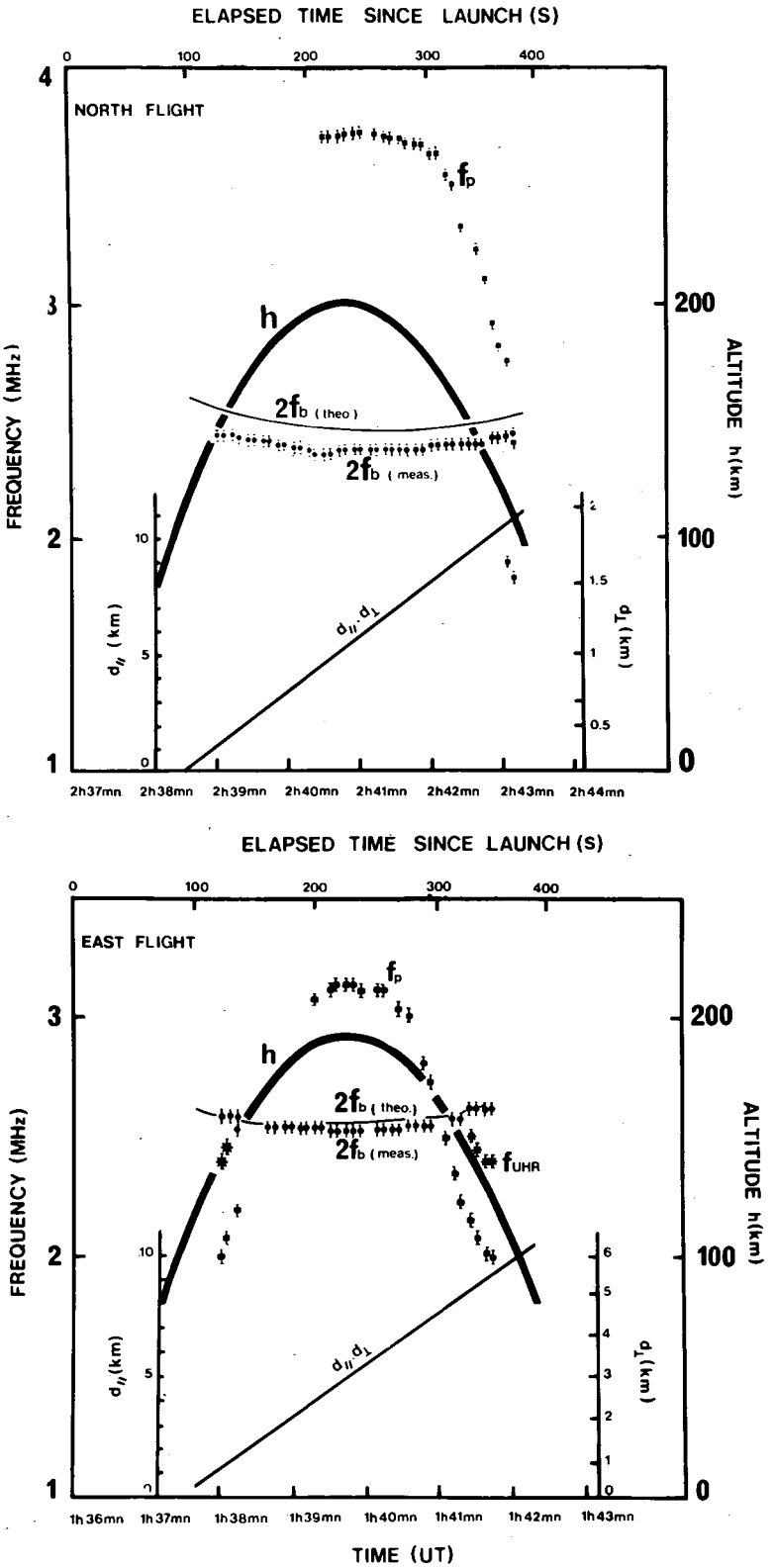

Fig. 4
Evolution of the resonances during both flights.

to an error on 2 f_b of the order of 10 kHz well inside the experimental uncertainties. We have used for this purpose the GSFC 12/66 model. It appears clearly that model and observational values are in good agreement during the East flight but that a discrepancy of about 100 kHz exists for the North flight.

After a careful examination this difference cannot be attributed to any experimental shift and thus must be considered as a diamagnetic effect likely due to the cesium plasma source. Let us remind in this connection, that a release of neutral gas of cesium takes place well before the creation of the plasma and remains after the end of the associated discharge.

2. *Electric field measurements*

Two methods were set up to measure the DC electric field (Delahaye *et al.*, 1978, Berthelier and Pirre, 1978). The first one uses the classical technique of the double sphere spinning with the rocket and the second measures the ion drift $\vec{V}_d = \vec{E} \wedge \vec{B}/\vec{B}^2$. As the second method is more tricky a special paper will be devoted to it in this issue, (Pirre *et al.*, 1980).

To ensure that the sheath impedance Z_s is small compared to the input impedance of the preamplifier (10 MΩ) the spheres are biased in such a way that Re $(Z_s) < 100$ kΩ.

The potential difference Φ between the two spheres, which is measured at the cone spin frequency, gives the apparent electric field (assumed to be perpendicular to the earth magnetic field)

$$\frac{\Phi \text{ measured}}{d} = \vec{E}_{\text{measured}} = \vec{E}_{\text{true}} + \vec{V}_{\text{cone}} \wedge \vec{B}$$

where d is the distance between the two spheres.

One spin period is needed to remove any offset which could appear between the two spheres ; thus we must wait for a period of time longer than 2 sec when no particular event occurs. This requirement restricts the data for the DC electric field to the periods of long pulses (2.56 sec) and the pauses of injection (2.56 sec). Tentatives to use half a period have given good results. The whole of the results for the North flight is drawn on Figure 5 in coordinates related to the earth magnetic field. Values of some tens of mVm^{-1} are coherent with the moderate magnetic activity already quoted ($K_p = 3^+$) which is generaly accompagnied by the penetration into the plasmasphere of strong magnetospheric electric fields (Stern, 1979).

It must be noted that the long pulses of the electron beam do not change perceptibly the behaviour of the electric field. This fact is clearly seen at the end of the North flight (Fig. 5) when the gun has worked regularly at 15 keV. However at this time, the perpendicular distance from the beam to the nose cone is rather large (> 1.5 km) and one might suspect another behaviour at the beginning of the flight, when this distance was smaller. Although the long pulses did not exist at this time,

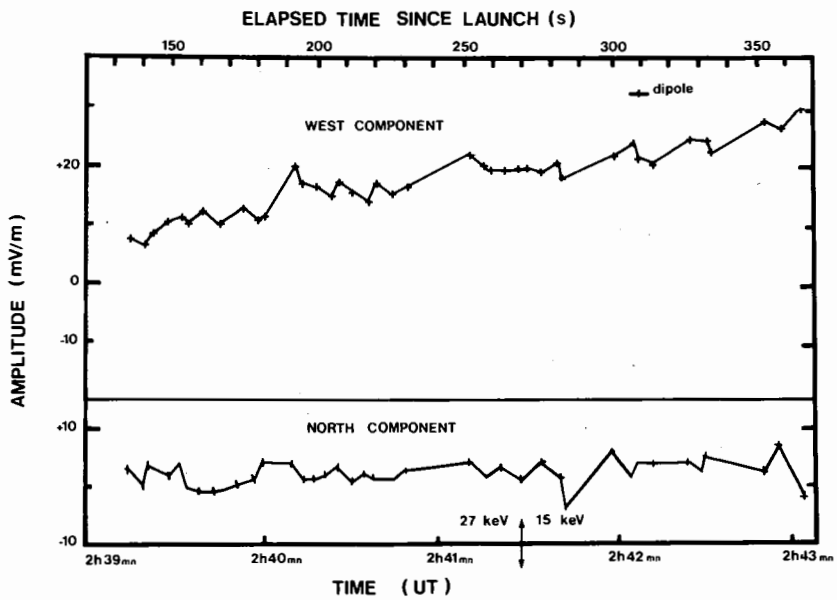

Fig. 5

DC electric field measured by the double spheres method in a geomagnetic frame of reference (Northward flight).

we can use the measurement of the amplitude of the electric component in the channel 10-50 Hz. In fact, during the short pulses (32 times 20 msec of injection followed by 20 msec of silence) if a polarization electric field is settled it must excite this channel at a 25 Hz frequency. No such event has been observed, even when the perpendicular distance is so low as 300 m, although the sensitivity of the channel is high (5 μV, see Table 1). It seems thus reasonable to state that the region of ion neutrality, if it exists, is confined very close to the beam.

An analogue conclusion holds if we consider the absence of any signal in the channel 10-50 Hz of the magnetic field. Its sensitivity of 3mγ (Table 1) leads to a threshold of detection at 500 m of 7.5 mA. It is thus well-founded to think that the return current is also confined along the electron beam in order to achieve a good balance of currents for an observer far from the beam.

3. Electronic temperature measurement

As previously quoted the spheres are biased in order to decrease the real part of the sheath impedance down to 100 kΩ ; it means that the current collected by the probe is mainly the electronic part inside the space charge region. Thus we can write the classical formula (Fahleson 1967)

$$I = 4\pi a^2 \, \mathrm{ne} \sqrt{\frac{KT}{2\pi m}} \exp\left(\frac{\mathrm{eV}}{KT}\right)$$

with obvious notation.

The differential resistance reads :

$$R_s = \frac{dV}{dI} = \frac{Kt}{eI}$$

The electronic temperature is thus deduced from the measurement of the sheath resistance by $T = 11.6\ IR_s$ where I, the bias current, is in μA and R_s in kΩ. If we restrict ourselves to the low frequency range (< 10 kHz) we can neglect the sheath capacitance and take $| Z_s | \approx R_s$. Finally we get in our case
$T = 1160\, I\,(g_1/g_2 - 1)$

Till 186 sec, at low altitudes (low electronic density) the current I is fixed at 1 μA which is a good value to measure the ionospheric temperature. After this time I is increased up to 8 μA, and the formula described above clearly indicates that it becomes very difficult to measure moderate value of electronic temperature. The sharp variation of the gain of the AGC within the VLF channel (0.5-10 kHz) induced by the commutation of the preamplifier input is taken as an estimator of the value of g_1/g_2

As we have performed the temperature measurement only once every two sequences, only four reliable values have been got and these are detailed in Table 2.

Table 2
Electronic temperature

Sequence	4	6	8	10
TIME H_0 + sec	107	133	158	184
Gun	NO	YES	NO	NO
$d_\perp$ m	190	360	570	750
Altitude km	128	156	176	191
Te °K	800	820	1 700	1 200

The values of the ionospheric temperature are quite normal (Sequence 4 and 10), and so is their increase with the altitude.

During the 6th sequence, fortunately, the long pulse (2.56sec) of the electron gun worked satisfactorily and the measurement of the temperature states that no thermal effects are visible at 360 m far from the beam.

The slight enlargment of T_e during the 8th sequence is likely due to a natural phenomenon which appears also by an intense noise just above the lower hybrid frequency (see below).

On board waves observations

In this paper, we will just describe the crude features of the waves emitted by the electron beam or other injections. So we will neglect the channel 10-100 kHz and restrict ourselves to the HF part of the frequency range (0.1-5 MHz) and to the VLF one (1-10 kHz). Some troubles during the East flight prevent us from presenting in a synthetic manner the data of this flight.

1. High frequency waves

The emissions in the frequency range 0.1-5 MHz during the North flight are displayed on the "sonagram" of Figure 6. At the bottom of this Figure a theoretical scheme of the gun sequence is drawn.

This sonagram arises from the swept frequency analyser which is calibrated periodically, so that black squares, regularly spaced, ranged on four harmonic levels (0.6, 1.8, 3.0, 4.2 MHz) are apparent. The vertical white lines correspond to the use of the SFA as part of the relaxation sounder. The change in the intensity of the background grey between the left and the right parts of this Figure is a consequence of the 20 dB commutation of the gain of the receiver. The trace ranging from 2 MHz up to 2.7 MHz before 2H 39 mm is due to the concomitant deployment of the dipole antenna and may be identified with a Langmuir wave.

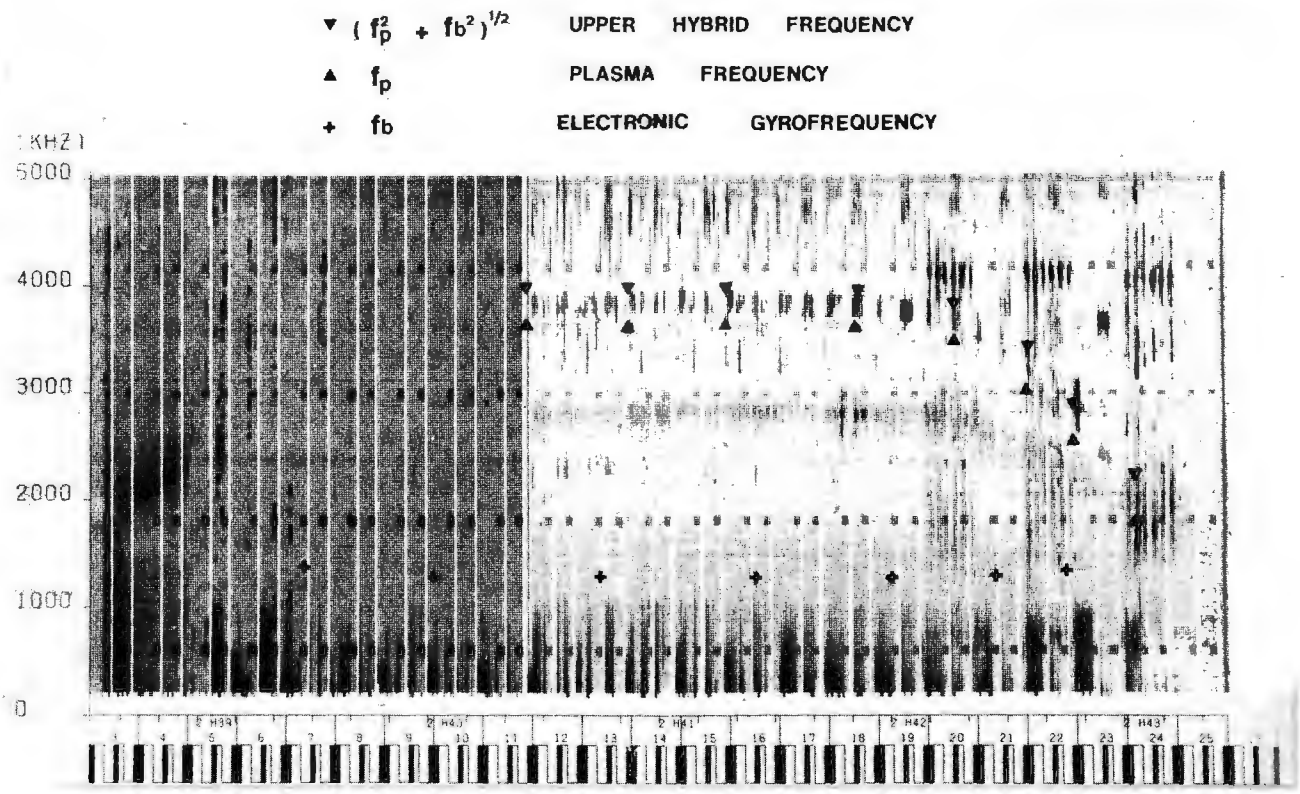

Fig. 6

High frequency waves observed during the North flight displayed like a sonagram (see text for details).

We have marked with special symbol the caracteristic frequencies of the ambient plasma (electronic gyrofrequency, plasma frequency, upper hybrid frequency). An analysis of Figure 6 reveals the presence of the following emissions :

– A large bandwith emission below the electronic gyrofrequency (≅ 1.2 MHz). It is always correlated with gun injection whatever the pulse duration.

Its temporal evolution follows exactly the evolution of the beam current. Its amplitude is rather large (1 mV) and provides the main energy radiated by the beam. Prolongation of this emission is seen only on the electric component of the LF frequency range (10 – 100 kHz) what seems to indicate an electrostatic character for this emission.

– A narrow band emission whose frequency is close to 3.8 MHz at the culmination and decreases along the descent of the nose cone. This emission is bounded by the plasma frequency and by the upper hybrid frequency. Its amplitude is moderate (200 μV) and lower than that of the whistler waves. While they are correlated with the electron beam injections it nevertheless exhibits a different temporal variation : a "pulsed emission" which reaches its maximum amplitude a few milliseconds after the beginning of an electron pulse and then decreases continuously to a background value. This behaviour explains why there is almost never a signal observed by the SFA during the long pulses.

– A narrow band emission, the middle frequency of which is close to the fourth harmonic of the electronic gyrofrequency ($4f_b \cong 4.8$ MHz). It seems to be correlated with the electron beam only during the short pulses but its weak amplitude (≅ 20 μV) makes difficult any temporal study. However, during the short pulses, the level is rather constant. We must note that no other harmonic of the electronic gyrofrequency has been recorded except during sequence 23 (pitch angle 70°) when a moderate signal (≅ 60 μV) near 3 f_b (≅ 3.6 MHz) was observed. This continuous emission occurs at a time which is remarkable : when the plasma frequency and the double of the electronic gyrofrequency are equal.

– A weak signal (30 μV) which in not related to the injection of the electron beam is clearly visible around 2.8 MHz near the culmination and its frequency decreases as the plasma frequency. This permanent emission cannot thus be attributed to an hardwave interference even if its origin is difficult to understand.

– Strong signals appear during sequences 20, 22 and 24. They are related neither to the electron gun performances nor to the cesium plasma source which is cut off

in the middle of sequence 20 but are present only when the broad band telemetry SPECTRUM is "on" ; it is why we consider it as their cause. Above the upper hybrid frequency there seems to be an harmonic structure, clearly visible during sequence 24 (2 MHz and 4 MHz). It is strongly modulated by the rotation of the nose cone at the spin frequency.

2. Very low frequency waves

In this frequency range, the electric component (0.5 – 10 kHz) and the magnetic component (1 – 10 kHz) were recorded with their waveform but alternately every 40 msec. Figure 7 shows the sonagram obtained numerically from the wave form of the electric component. As in Figure 6, a theoretical scheme of the gun sequence is drawn at the bottom and the vertical white lines correspond to the performances of the relaxation sounder.

Five groups of phenomena can be distinguished.

– Up to 2 kHz a permanent signal is recorded on both components and its fine structure proves that it is a dawn chorus.

– An intense electrostatic noise between 6.5 and 9 kHz which is of natural origin and appears like three puffs during sequences 7,8 and 9.

– A monochromatic signal visible only on the electric part whose frequency is close to 4.5 kHz at the culmination and which decreases according to the descent of the nose cone. This emission appears when the bias current of the spheres has grown up to 8 μA and ceases when the plasma source is cut off. Furthermore this signal is modulated at the spin frequency of the nose cone, what is quite unexpected.

– A large band emission which ranges from 10 kHz down to few kHz (generally the previous frequency plays the role of a cut off frequency). This emission is seen very seldom on the magnetic component (sequences 12, 14) and is likely the continuation of the whistlers waves previously described.

– Discrete monochromatic emissions well correlated with the gun operation. Values of their frequency (6.7 kHz, 5 kHz, 4 kHz, etc. . .) are difficult to interpret but it is sure that up to sequence 7 the electron beam has produced waves at its frequency of modulation (2 kHz) and its harmonics (4 – 6 kHz).

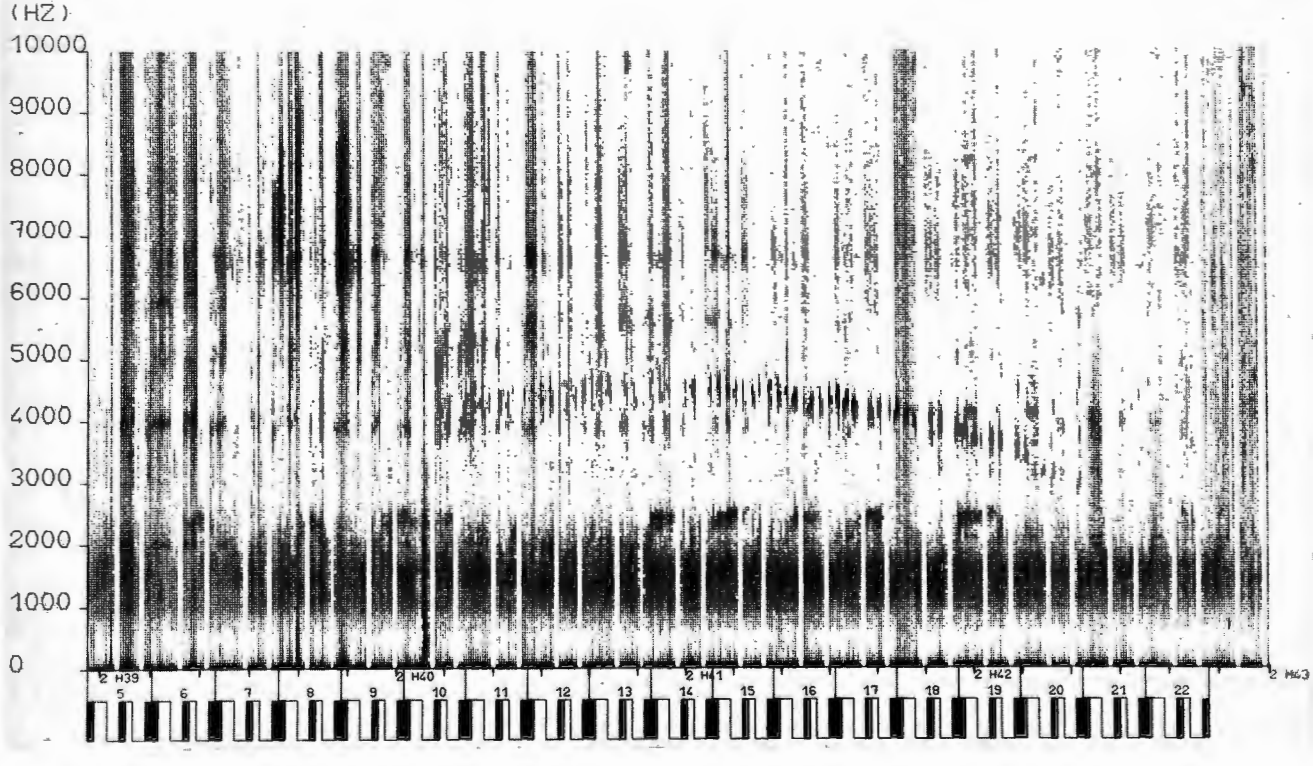

Fig. 7

Very low frequency waves observed during the North flight on the electric component displayed like a sonagram (see text for details).

Conclusion

It is beyond the scope of this paper to discuss even in a crude manner the physical processes which are responsible for all the observed emissions. But we would stress that many new features of the interaction of an electron beam and the ionospheric plasma have been revealed and that comparison with previous data (e.g. Electron Echo Experiment) will give us a deeper insight in the involved physical mechanisms. Results of these comparison are presented in the following papers.

References

Berthelier J.J., M. Pirre, "Ion Analysers for measurement of D.C. electric field and ion temperature" *Space. Sci. Inst.* **4,** (2-3), 213-226, 1978.

Delahaye J.Y., J. Lavergnat, R. Ney, J.F. Karczewski, "Wave measurements in the ARAKS experiment" *Space. Sci. Inst.,* **4,** (2-3), 143-169, 1978.

Fahleson U., "Theory of electric field measurements conducted in the magnetosphere with electric probes" *Space. Sci. Rev.,* 7, 238-262, 1967.

Gusev G.A., I.A. Zhulin, Yu'V. Kushnerevsky, V.V. Migulin, S.A. Pulinets, "Broad-band wave measurements in the ARAKS experiment" *Space Sci. Instr.,* **4,** (2-3), 171-176, 1978.

Mishin E.V., Yu.Ya. Ruzhin, "The dynamics of HF radio emission in the Araks experiments" *Annales de Géophysique,* 1980 ; this issue.

Petit M., J. Bitoun, P. Graff, R. Feldstein, B. Higel "Ondes de plasma à vitesse de groupe faible" *Ann. Telec.,* **27,** (9-10), 417-429, 1972.

Pirre M., J.J. Berthelier, "Ion drift velocity measurements on the nose cone during the first ARAKS experiment", *Ann. de Geophys.,* 1980 (this issue).

Stern D.P., "The electric field and global electrodynamics of the magnetosphere", *Reviews of Geophys. and Space, Phys.,* **17,** 4, 626-640, 1979.